Isolation, Characterization, and Environmental Application of Bio-Based Materials as Auxiliaries in Photocatalytic Processes

Davide Palma [1,2], Alessandra Bianco Prevot [2,*] , Luisella Celi [3], Maria Martin [3], Debora Fabbri [2], Giuliana Magnacca [2,4], Michele R. Chierotti [2] and Roberto Nisticò [5,*]

[1] CNRS, Institut de Chimie de Clermont-Ferrand (ICCF)-Campus Universitaire des Cézeaux, 24 Avenue Blaise Pascal, 63178 Aubiere CEDEX, France; davide.palma@edu.unito.it

[2] Department of Chemistry, University of Torino, Via P. Giuria 7, 10125 Torino, Italy; debora.fabbri@unito.it (D.F.); giuliana.magnacca@unito.it (G.M.); michele.chierotti@unito.it (M.R.C.)

[3] Department of Agricultural, Forest and Food Sciences, Soil Biogeochemistry, University of Torino, Largo Paolo Braccini 2, 10095 Grugliasco, Italy; luisella.celi@unito.it (L.C.); maria.martin@unito.it (M.M.)

[4] Nanostructured Interphases and Surfaces (NIS) Centre, Via P. Giuria 7, 10125 Torino, Italy

[5] Department of Applied Science and Technology DISAT, Polytechnic of Torino, C.so Duca Degli Abruzzi 24, 10129 Torino, Italy

* Correspondence: alessandra.biancoprevot@unito.it (A.B.P.); roberto.nistico@polito.it (R.N.); Tel.: +39-011-670-5297 (A.B.P.); +39-011-090-4762 (R.N.)

Abstract: Sustainable alternative substrates for advanced applications represent an increasing field of research that attracts the attention of worldwide experts (in accordance with green chemistry principles). In this context, bio-based substances (BBS) isolated from urban composted biowaste were purified and characterized. Additionally, these materials were tested as auxiliaries in advanced oxidizing photocatalytic processes for the abatement of organic contaminants in aqueous medium. Results highlighted the capability of these substances to enhance efficiency in water remediation treatments under mild conditions, favoring the entire light-driven photocatalytic process.

1. Introduction

The exploitation of renewable resources as an alternative feedstock for the production of value-added bio-based chemicals and materials has dramatically increased in recent decades [1–10]. Among the different substrates, the use of an organic fraction from urban and/or agricultural waste has attracted the attention of experts driven by the principles of a circular (and sustainable) economy ([11,12] and references therein). Furthermore, the current principal environmental exploitation of biowaste (intended as: biodegradable garden and park waste, food and kitchen waste from households, restaurants, caterers, and retail premises, and comparable waste from food processing plants) in the European Union (EU) is the production of methane (a greenhouse gas) from decomposing processes in landfills [3,13]. In 1999, the Landfill Directive of the European Community (1999/31/EC) forced all EU member states to diminish the amount of biodegradable municipal waste left in landfill, with the aim of promoting their re-use and recycling [14].

In order to follow the EU dictates, several studies in this topic are involved in the valorization of biowaste as starting materials for the production of new value-added products, such as fine chemicals [15–17], polymeric (mostly bioplastics) and composite materials [4,18–21], carbonaceous

materials and biochars [22–25], biofuels, and/or biogas [26–30]. In this context, composting consists of an (an)aerobic biological process for decomposing the organic fraction into a more stabilized material with different properties that depend on the initial composition [11] and composting methodologies.

Seeking further biowaste valorization, waste-derived bio-based substances (BBS in the following) have been isolated from urban-composted biowaste; BBS are supramolecular aggregates with a complex lignin-derived structure (similar to soil humic substances) containing several functionalities (namely, acid and basic functional groups bonded to aromatic and aliphatic chains) [31–35]. The presence of both hydrophilic and hydrophobic functionalities forming the chemical structure of such BBS confers to these substances amphiphilic properties, as testified by the literature on analogous substrates [36–38]. As reported in our previous study [39], these BBS can be used in several industrial applications (as emulsifiers, foaming agents, in detergent formulations or as textiles auxiliaries, for the production of nanostructured materials, in animal husbandry, as fertilizers, or for the production of biofuels and bioplastics). Among the potential applications of such BBS, the most striking one is the "waste for cleaning waste" [40]. This approach implies the use of BBS as chemical auxiliaries for the photochemical degradation of pollutants in aqueous environment. According to the literature, these BBS have been used (either in homogeneous or heterogeneous phase) to sensitize the photodegradation of standard contaminants as well as emerging pollutants (EPs), whose dangerousness has only recently been recognized [41,42].

Advanced oxidation processes (AOPs) have been widely studied as a sustainable alternative treatment for the purification of the contaminated aqueous environment [43–46]. Among these, (photo)-Fenton processes (in the presence of a Fe(II) source, H_2O_2, and eventually UV irradiation) have been widely studied as a greener alternative to the more conventional methods for remediation of contaminated wastewaters [47]. The Fenton reaction provides the degradation of organic contaminants by means of oxidizing species (principally hydroxyl radicals (OH)) formed by H_2O_2 decomposition catalyzed by Fe(II). Additionally, the Fenton process can be accelerated by UV-Visible irradiation (i.e., $\lambda < 500$ nm, thus becoming a photo-Fenton process) [48,49]. The introduction of humic-like substances in (photo)-Fenton processes has been reported to enhance the degradation of organic pollutants by direct formation of different O-containing reactive species (i.e., hydroxyl radicals, superoxide species, and singlet oxygen) or by involving the triplet-excited states of the functionalities still present in the humic-like structure [50,51]. On the other hand, humic-like substances can accelerate the Fe(III)-to-Fe(II) redox mechanism, thus regenerating the catalyst [52].

Therefore, this study aims at isolating humic- and fulvic-like substances (BBS-HA and BBS-FA) obtained from green composted biowaste (GC in the following) and characterizing the physicochemical properties in order to elucidate the structural organization and the surfactant behavior as well as their photocatalytic performance on homogeneous degradation processes, simulating the remediation of a contaminated wastewater.

2. Results and Discussion

2.1. Spectroscopic and Analytical Characterization of BBS-HA

The two fractions obtained from the compost, BBS-HA and BBS-FA, were characterized by spectroscopic and chemical analyses. Specific ultraviolet absorbance (SUVA) values, obtained by normalizing the absorbance at 254 nm by the DOC content, were 4.71 and 4.54 L mg^{-1} m^{-1} for BBS-HA and BBS-FA, respectively, indicating that both components have a high aromatic character [53,54].

FT-infrared spectra of BBS-HA and BBS-FA (Figure 1) present the following bands: (i) a broad peak at ca. 3400 cm^{-1} attributable to O–H stretching vibrational mode; (ii) shoulder peaks at ca. 2940–2920 cm^{-1} and 2850 cm^{-1} due to both asymmetric and symmetric aliphatic C-H stretching mode; (iii) a band at ca. 1750–1700 cm^{-1} due to C=O stretching mode of carbonyl functionalities (mainly carboxylic acids, see Figure 1, red circles), more pronounced in BBS-FA; (iv) signals at ca. 1650–1630 cm^{-1} attributable to aromatic C=C skeletal vibrations (Figure 1, black squares), more

pronounced in BBS-HA than in BBS-FA; (v) a broad band at 1420–1410 cm^{-1} assigned to both O–H deformation and C–O stretching modes of phenolic moieties (Figure 1, red circles); (vi) an intense band at 1230–1220 cm^{-1} due to both C–O stretching and O–H deformation modes of COOH groups (Figure 1, red circles). The band in the 1040–1030 cm^{-1} range is attributed to C–O stretching of polysaccharides and polysaccharide-like impurities (i.e., residues of the non-humic fraction, Figure 1, white circles) [55]. Interestingly, the BBS-HA presents also a shoulder at ca. 1545–1540 cm^{-1} belonging to the aromatic C=C stretching mode and/or to secondary amide [56] (Figure 1, black squares), and a sharp (but weak) signal at ca. 1130 cm^{-1} attributable to C–O stretching vibration modes due to alcoholic and ether functionalities (Figure 1, black star). The interpretation of spectra was according to the literature [55,56]. Thus, BBS-HA appeared to be characterized by a higher aromatic character, in agreement with SUVA findings, and by the incorporation of proteinaceous residues. As expected by the extraction method, the BBS-FA fraction has a higher amount of carboxyl groups [55,56].
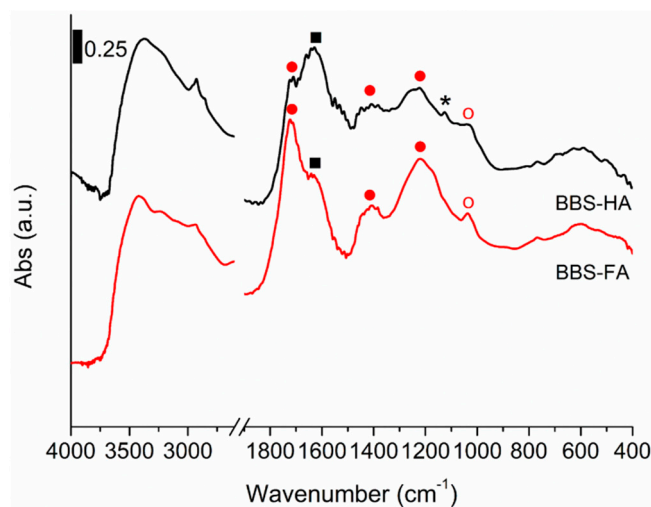

Figure 1. Absorbance FTIR spectra in the 4000–400 cm^{-1} range of BBS-HA (solid black curve), and BBS-FA (solid red curve). The main relevant peaks are labeled. Legend: aromatic C=C (black square), O-containing functional groups (red circle), polysaccharide-like impurities (white circle), and alcoholic/ether C–O (black star).

[13]C solid-state nuclear magnetic resonance (NMR) spectroscopy offers the possibility of direct chemical characterization of organic materials in terms of content of different functional groups [57–59]. In the ^{13}C CPMAS solid-state NMR spectrum of BBS-HA (Figure 2 together with the deducted abundance of functional groups), the region between 160 and 220 ppm is dominated by a signal at 173 ppm, due to carboxyl C. The aromatic and phenolic region (110–160 ppm) represented 30% of C. Here, the signal at 129 ppm, indicating a relatively larger presence of non-substituted aromatic rings, may be due to aromatic lignin [60]. Weaker signals occurred in the 45–110 ppm region, which included only 13% of C. The signal at 71 ppm is associated to the simultaneous resonance of C-2, C-3, and C-5 of pyranoside rings in cellulose and hemicellulose [56], while the weak signals at 65 ppm (C-6) and 105 ppm (anomeric C) indicated a low presence of crystalline cellulose. The high signal at 56 ppm is attributable to lignin methoxyl C and highlights the selective enrichment of lignin-derived compounds with composting as a result of cellulose decomposition. The 0–45 ppm region is characterized by two signals at 30 and 24 ppm, most likely attributable to paraffinic C of lipids and waxes. Their integration area almost equals that of the aromatic region (28.8%) and again derives from the selective enrichment of recalcitrant components [60].
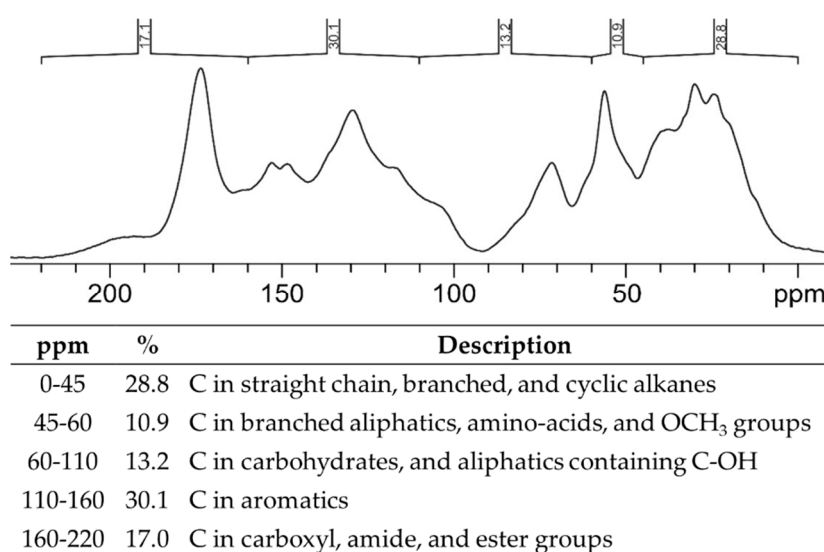
ppm	%	Description
0–45	28.8	C in straight chain, branched, and cyclic alkanes
45–60	10.9	C in branched aliphatics, amino-acids, and OCH_3 groups
60–110	13.2	C in carbohydrates, and aliphatics containing C-OH
110–160	30.1	C in aromatics
160–220	17.0	C in carboxyl, amide, and ester groups

Figure 2. ^{13}C CPMAS solid-state NMR spectrum of BBS-HA (**top**), assignments and relative area calculated from the NMR spectrum (**bottom**).

Surface tension measurements of BBS-HA in the 0.2 to 5.0 g L^{-1} concentration range evidenced a trend to decrease when increasing the BBS-HA concentration, thus clearly indicating that BBS-HA had marked surfactant behavior (Figure 3). Nonetheless, conversely to the behavior reported for analogous substances [61], no evident discontinuities were observed, attributable to a variation of the microstructure, following the formation of micellar aggregates. Micelles could influence solute properties depending on the substrate partitioning between the bulk solution and the micellar phase; a net change of the surface reactivity with solute species, due to the formation of micellar aggregates, has been reported for humic acids structurally similar to BBS-HA [62]. Moreover, the presence of a surfactant, even if below its critical micellar concentration, could enhance the solubility in water hydrophobic substrates. In the present case we do not expect any peculiar behavior related to a specific BBS-HA microstructure depending on the concentration; on the other hand, the high UV-VIS light absorption coefficient of BBS-HA could result in a screen effect for its photochemical application (see BBS-HA UV-Vis spectrum reported in Figure 4). Based on this latter aspect, an upper BBS-HA concentration limit of 1.0 g L^{-1} was chosen to study the photocatalytic performance of BBS-HA.
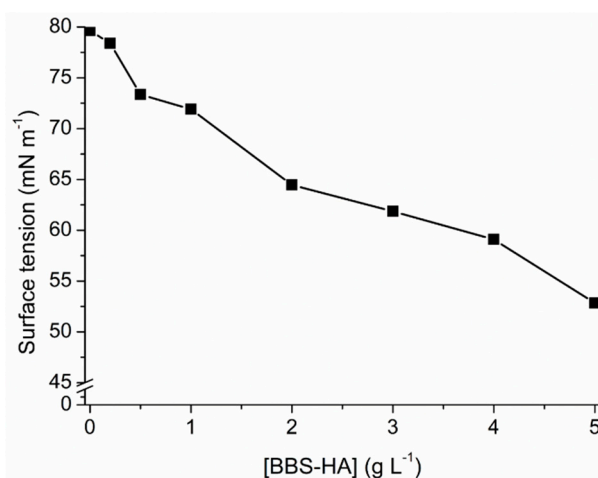

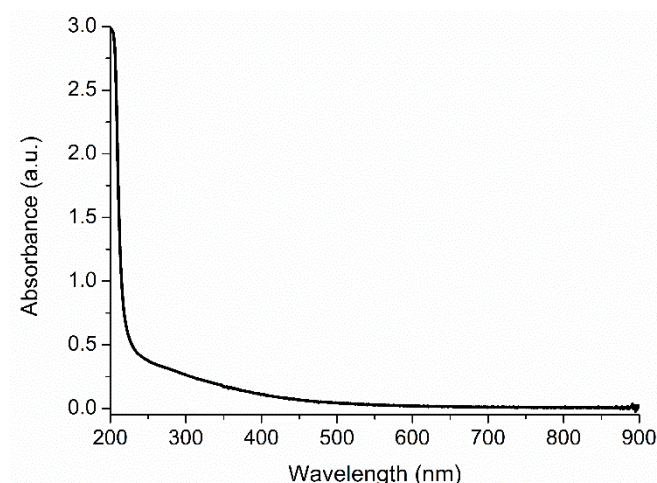**Figure 3.** Surface tension vs. BBS-HA concentration.

Figure 4. UV-VIS absorption spectrum in the 200–900 nm range of an aqueous solution containing 0.01 g L^{-1} of BBS-HA.

2.2. Photocatalytic Performances of BBS-HA in Homogeneous Phase

The capability of BBS-HA to promote the photodegradation of organic pollutants has been tested using caffeine, a substance naturally occurring in some beverages and also used as a pharmacological agent, as a probe molecule, being included in the list of contaminants of emerging concerns (CECs). Preliminary experiments were performed by irradiating an aqueous solution of caffeine (5 mg L^{-1}) in the presence of different amounts of dissolved BBS-HA (from 0.1 to 1.0 g L^{-1}). The pH was not modified and was in the range 8.0–8.5; this slightly basic pH originates from the preparation of the BBS-HA solutions at different concentrations, obtained by diluting the BBS-HA stock solution having a pH value in the range 9.0–9.5 (see Section 3.3). The results indicated that even after several hours of irradiation (up to 6 h), the maximum yield of caffeine degradation reached 10%. Based on these data, further experiments were performed lowering the pH at a value of 5.5, and comparing the results obtained by irradiating the caffeine in the presence of (i) BBS-HA alone; (ii) BBS-HA and hydrogen peroxide; (iii) BBS-HA, hydrogen peroxide and Fe(II) (photo-Fenton like). This mild, circumneutral pH was chosen on the basis of encouraging results reported in analogous experiments performed in the presence of other waste-sourced biosubstances [63]. Figure 5 reports the obtained results; in the panel A, the relative caffeine concentration evolution with irradiation time is reported for the three experimental conditions explored. When the irradiation is performed in the presence of BBS-HA alone, a very low caffeine decrease can be observed, yielding about 10% of caffeine abatement after 6 h of irradiation. It is reasonable to attribute this low but not negligible degradation to the BBS-HA capability of generating reactive oxygenated species upon irradiation, similar to what has been previously reported [64]. Upon the addition of hydrogen peroxide, a significant enhancement of the caffeine degradation rate occurs, and after 6 h of irradiation, ca. 75% of caffeine has been degraded. However, the photo-Fenton process performed in the presence of BBS-HA is dramatically faster; for this reason, in this latter condition, a shorter reaction time was explored and the observed caffeine degradation profile is reported in panel B (Figure 5): The complete disappearance of caffeine was already observed after 10 min; this result is in agreement with the literature [63], where a group of emerging contaminants was subjected to photo-Fenton treatment in the presence of a similar BBS. The positive effect of the present BBS-HA on the photo-Fenton process can be ascribed to the formation of Fe(II)—BBS-HA complexes, which may react more rapidly with H_2O_2 than Fe(II)—aquo complexes, leading to a higher rate of HO• production. Voelker and Sulzberger [65] observed the same mechanism with fulvic acids, concluding that Fe(II)—fulvate complexes formed at pH = 5 accelerated the Fenton reaction. Using iron complexing substances in order to promote photo-Fenton processes

under milder pH values is indeed a topic attracting attention from many researchers and recently the use of Ethylenediamine-*N*,*N'*-disuccinic acid (EDDS) was proposed [66].
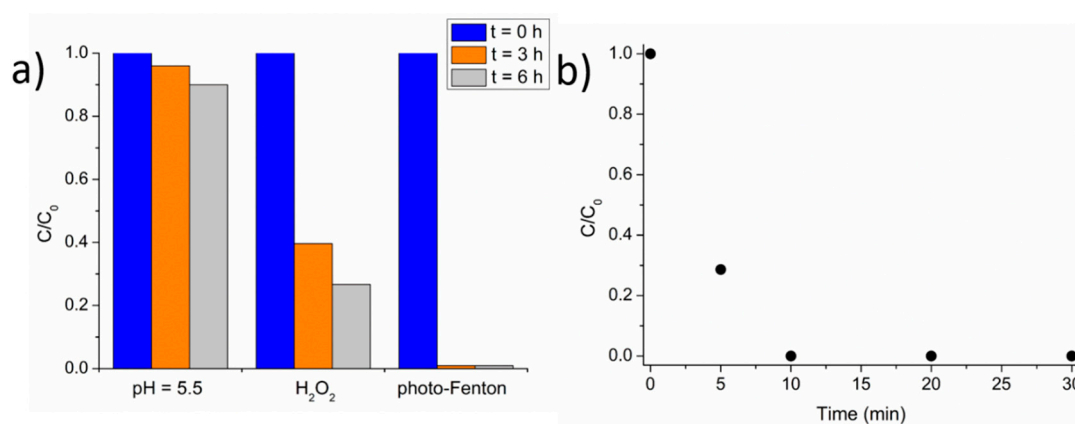

Figure 5. (**a**) Relative caffeine concentration evolution with time, under irradiation in different conditions. Initial caffeine concentration 5 mg L^{-1}; BBS-HA added 0.1 g L^{-1}. Additional reagents: histograms labelled H_2O_2, addition of 1.5×10^{-3} mol L^{-1} of H_2O_2; histograms labelled photo-Fenton, addition of 1.5×10^{-3} mol L^{-1} of H_2O_2 and 5.0 mg L^{-1} of iron(II). (**b**) Relative caffeine concentration evolution with time in photo-Fenton conditions. Initial caffeine concentration 5 mg L^{-1}; BBA-HA concentration 0.1 g L^{-1}; concentration of H_2O_2 1.5×10^{-3} mol L^{-1} and concentration of iron(II) 5.0 mg L^{-1}.

3. Materials and Methods

3.1. Materials

Bio-based substances (BBS) were isolated from commercially composted urban biowaste, obtained from the *ACEA Pinerolese Industriale S.p.A.* waste treatment plant in Pinerolo (Pinerolo, Italy). The composted biowaste is derived from urban public park trimmings and home gardening residues aged for more than 180 days. During this time, the fraction of aromatic C and –COOH functionalities increase, while the fraction of aliphatic, easily degradable organic molecules decreases [33]. The process is an advanced system that comprises specific technological facilities, developed by *ACEA Pinerolese Industriale S.p.A*, and under European validation [67]. The physicochemical properties of the starting compost are reported in Table 1.

Table 1. Physicochemical parameters of the green compost (GC).

Property	Unit	Value
pH	-	7.0
Moisture content	%	50
Total organic C	%	20
Total organic N	%	0.8
C/N ratio	-	25
EC	mS cm^{-1}	1.8

Other reagents used are: sodium hydroxide (NaOH, purity $\geq$ 98.0%, CAS 1310-73-2, Sigma-Aldrich, Saint Louis, MO, USA), hydrochloric acid (HCl, conc. 37 wt %, CAS 7647-01-0, Sigma-Aldrich, Saint Louis, MO, USA), anhydrous potassium chloride (KCl, purity $\geq$ 99.0%, CAS 7447-40-7, Sigma-Aldrich, Saint Louis, MO, USA), polyvinylpyrrolidone (PVP, CAS 25249-54-1, Sigma-Aldrich, Saint Louis, MO, USA), amberlite (CAS 9002-23-7, Sigma-Aldrich, Saint Louis, MO, USA), caffeine (CAS 58-08-2, Sigma-Aldrich, Saint Louis, MO, USA), H_2O_2 (CAS 7722-84-1,

Sigma-Aldrich, Saint Louis, MO, USA). All aqueous solutions were prepared using ultrapure water Millipore Milli-Q^{TM}. All chemicals were used without further purification.

3.2. Compost Fractionation and BBS Recovery

The compost fractionation is a modified version of the procedure adopted for the separation of humic and fulvic acids from soils and organic matrices, proposed by the *International Humic Substance Society* [68]. In detail, the compost was dispersed into a 0.5 M NaOH solution in polyethylene (PE) bottles with 1:10 solid:solution ratio, and left under mechanical shaking in the dark overnight under an atmosphere of N_2. The supernatant (that contains the BBS fractions) was then separated from the solid residue by centrifugation at 3000 rpm for 15 min, filtered and newly centrifuged at 10,000 rpm for 10 min to finely remove the solid particles still present in the supernatant. The latter was again filtered at 2.7 μm. The pH was corrected at pH < 1 by adding HCl conc. to promote the flocculation of the humic-like substances and the flask maintained in the dark overnight. The day after, the suspension was again centrifuged at 10,000 rpm for 20 min to separate the precipitate (humic-like substances) from the supernatant (still containing the fulvic-like substances). Finally, the supernatant was filtered again, collected in PE bottle, and kept under N_2 atmosphere at 4 °C.

The humic-like fraction was purified from the NaCl content (due to the previous acid-base treatments and pH adjustments) by cyclic washing with deionized H_2O, followed by centrifugation (rate: 10,000 rpm, time: 10 min), until pH 3 was reached. The humic-like fraction was then dialyzed against deionized water in tubular membranes (*Spectra/Por*® *6*, cut-off: 1000 Da, thus recovering only BBS with a M_W higher than 1000 Da) for 3–4 days with daily water replenishments until reaching an electrical conductivity below 10 μS cm^{-1}. The suspension was then freeze-dried and kept as such for further analysis. The obtained fraction was coded as BBS-HA, where HA stands for Humic-Acid.

The fulvic-like fraction present in the supernatant was separated from the non-humic soluble components (peptides and carbohydrates residues), through a first column purification with PVP (elution rate: 1–2 mL min^{-1}) that retained the fulvic-like substances, discharging the non-humic fraction. The fulvic like substances were eluted from the column with 0.1 N NaOH, and then purified through elution in an amberlite column (H$^+$-saturated cation-exchange resin) for the removal of Na$^+$. In order to obtain a solid substrate, the fulvic-like fraction was freeze dried and then completely dried in an oven at 40 °C. This type of BBS were coded as BBS-FA, where FA stands for Fulvic-Acid.

This procedure yielded 22 g of BBS-HA and 1 g of BBS-FA every 1000 g of compost. Thus, due to the very low separation yield of BBS-FA from this compost, BBS-HA were the only bio-based material considered as photocatalytic auxiliaries for testing possible applications in the photodegradation of organic molecules.

3.3. Physicochemical and Photocatalytic Characterization

A stock 5 g L^{-1} BBS-HA aqueous solution was prepared by taking up solid BBS-HA with MilliQ$^®$ water, stirring 1 h, then adding aliquots 0.2 M NaOH to keep pH in the 9.0–9.5 range until the complete solid dissolution occurred. The solution was finally filtered through a 0.45 μm Millex–HA membrane (Millipore, Merk, Darmstadt, Germany) and brought to the required volume with MilliQ$^®$ water. The stock solution was kept frozen before use. Aliquots of the stock solution were diluted with MilliQ$^®$ water to obtain solutions containing variable amounts of BBS-HA. UV—visible absorbance measurements were performed on a Helios (Thermo Electron, Waltham, MA, USA) spectrophotometer with deionized water as the blank. A quartz cell with 1.0 cm path length was used, and analyses were performed at room temperature. Dissolved organic carbon (DOC) measurements were performed using Pt-catalyzed, high-temperature combustion (850 °C) followed by infrared detection of CO_2 by means of a VarioTOC (Elementar, Hanau, Germany) [53]. Specific ultraviolet absorbance (SUVA) values were determined by normalizing the UV absorbance measured at λ = 254 nm by the DOC concentration and are reported in the units of liter per milligram carbon per meter (L mg^{-1} m^{-1}) [54].

Fourier transform infrared (FTIR) spectra were recorded in transmission mode by means of a Bruker Vector 22 spectrophotometer (Billerica, MA, USA) equipped with Globar source, DTGS detector, and working with 128 scans at 4 cm^{-1} resolution in the 4000–400 cm^{-1} range. Samples were mixed with KBr (1:20 wt. ratio).

Solid-state NMR spectrum of BBS-HA was collected on a Bruker Avance II 400 Ultra Shield instrument, working at 400.23 and 100.63 MHz for ^{1}H and ^{13}C, respectively. The sample was packed in a cylindrical zirconia rotor (4 mm o.d.), with a sample volume of 80 μL and spun at 12 kHz to minimize the spinning sidebands. The experiment employed the ramp CP pulse sequence (^{1}H 90° pulse = 3.6 μs; contact time = 1 ms) with the TPPM ^{1}H decoupling (rf field = 69.4 kHz) during the acquisition period. 400,000 scans were accumulated with an optimized relaxation delay of 0.2 s. The spectrum was processed with a line broadening of 50 Hz. The ^{13}C chemical shift scale was referenced with the resonance of α-glycine (^{13}C methylene signal at 43.5 ppm), which was used as an external standard.

Surface tension measurements were performed with a digital tensiometer (K10, Krüss, Hamburg, Germany) equipped with a platinum Wilhelmy plate.

Photodegradation experiments were carried out by irradiating, under continuous stirring, 10 mL of aqueous samples in a closed Pyrex® cell with a Xenon (1500 W) lamp (Solarbox, CO.FO.ME.GRA S.r.l., Milan, Italy) equipped with a 340 nm cut-off filter. The irradiance of the lamp, measured with a UV-Multimeter system, was 26.7 W m^{-2}. The caffeine degradation was monitored by HPLC, employing a Merck-Hitachi instrument, equipped with Lichrospher RP-C18 (125 mm × 4 mm i.d., particle diameter = 5 μm, from Merck, Darmstadt, Germany), L-6200 pumps and UV/Vis L-4200 detector. The selected eluent was a 1% H_3PO_4 in 50/50 (vol %) methanol/water mixture at 0.8 mL min^{-1} constant flow. The caffeine detection wavelength employed was 275 nm. Photo-catalytic trials were performed in different experimental conditions: in the presence of (i) BBS-HA alone; (ii) BBS-HA and H_2O_2; (iii) BBS-HA, H_2O_2 and $FeSO_4 \cdot 7H_2O$ (photo-Fenton like).

4. Conclusions

Composted waste-derived bio-based substances (BBS-HA) were isolated and characterized physicochemically. The obtained materials, showing amphiphilic properties, were used as auxiliaries in photodegradation processes for the abatement of caffeine (the target contaminant) in aqueous medium. Results obtained evidenced the promising capability of these substances to drive photo-Fenton-like processes for water treatments under mild conditions, making the exploitation of these biowaste-derived substances extremely powerful and interesting from the industrial viewpoint. In fact, the introduction of such BBS in light-driven photocatalytic processes provides an overall enhancement of the environmental and economic sustainability of the entire process, in accordance to the "waste cleaning waste" philosophy and the green chemistry principles. Based on these preliminary encouraging results, further investigation aiming to give insights into the key reactive species and the key degradation reactions deserves to be undertaken.

Conflicts of Interest: The authors declare no conflict of interest. The founding sponsors had no role in the design of the study; in the collection, analyses, or interpretation of data; in the writing of the manuscript, and in the decision to publish the results.

References

1. Kerton, F.M.; Liu, Y.; Omari, K.W.; Hawboldt, K. Green chemistry and the ocean-based biorefinery. *Green Chem.* **2013**, *15*, 860–871. [CrossRef]
2. Thomsen, M.; Seghetta, M.; Mikkelsen, M.H.; Gyldenkærne, S.; Becker, T.; Caro, D.; Frederiksen, P. Comparative life cycle assessment of biowaste to resource management systems—A Danish case study. *J. Clean. Prod.* **2017**, *142*, 4050–4058. [CrossRef]
3. Nisticò, R. Aquatic-derived biomaterials for a sustainable future: A European opportunity. *Resources* **2017**, *6*, 65. [CrossRef]
4. Brockhaus, S.; Petersen, M.; Kersten, W. A crossroads for bioplastics: Exploring product developers' challenges to move beyond petroleum-based plastics. *J. Clean. Prod.* **2016**, *127*, 84–95. [CrossRef]
5. Kai, D.; Tan, M.J.; Chee, P.L.; Chua, Y.K.; Yap, Y.L.; Loh, X.J. Towards lignin-based functional materials in a sustainable world. *Green Chem.* **2016**, *18*, 1175–1200. [CrossRef]
6. Isikgor, F.H.; Remzi Becer, C. Lignocellulosic biomass: A sustainable platform for the production of bio-based chemicals and polymers. *Polym. Chem.* **2015**, *6*, 4497–4559. [CrossRef]
7. Nisticò, R.; Evon, P.; Labonne, L.; Vaca-Medina, G.; Montoneri, E.; Vaca-Garcia, C.; Negre, M. Post-harvest tomato plants and urban food wastes for manufacturing plastic films. *J. Clean. Prod.* **2017**, *167*, 68–74. [CrossRef]
8. Arshadi, M.; Attard, T.M.; Bogel-Lukasik, R.; Brncic, M.; da Costa Lopes, A.M.; Finell, M.; Geladi, P.; Gerschenson, L.N.; Gogus, F.; Herrero, M.; et al. Pre-treatment and extraction techniques for recovery of added value compounds from wastes throughout the agri-food chain. *Green Chem.* **2016**, *18*, 6160–6204. [CrossRef]
9. Eggleston, G.; Lima, I. Sustainability issues and opportunities in the sugar and sugar-bioproduct industries. *Sustainability* **2015**, *7*, 12209–12235. [CrossRef]
10. Nisticò, R.; Franzoso, F.; Cesano, F.; Scarano, D.; Magnacca, G.; Parolo, M.E.; Carlos, L. Chitosan-derived iron oxide systems for magnetically guided and efficient water purification processes from polycyclic aromatic hydrocarbons. *ACS Sustain. Chem. Eng.* **2017**, *5*, 793–801. [CrossRef]
11. O'Callaghan, K. Technologies for the utilisation of biogenic waste in the bioeconomy. *Food Chem.* **2016**, *198*, 2–11. [CrossRef] [PubMed]
12. Girotto, F.; Alibardi, L.; Cossu, R. Food waste generation and industrial uses: A review. *Waste Manag.* **2015**, *45*, 32–41. [CrossRef] [PubMed]
13. Biodegradable Waste. Available online: http://ec.europa.eu/environment/waste/compost/index.htm (accessed on 11 October 2017).
14. Waste. Introduction. Available online: http://ec.europa.eu/environment/waste/landfill_index.htm (accessed on 22 November 2017).
15. Shamsul, N.S.; Kamarudin, S.K.; Rahman, N.A. Study on the physical and chemical composition of agro wastes for the production of 5-hydroxymethylfurfural. *Bioresour. Technol.* **2018**, *247*, 821–828. [CrossRef]
16. Matharu, A.S.; de Melo, E.M.; Houghton, J.A. Opportunity for high value-added chemicals from food supply chain wastes. *Bioresour. Technol.* **2016**, *215*, 123–130. [CrossRef] [PubMed]
17. Yang, X.; Choi, H.S.; Park, C.; Kim, S.W. Current states and prospects of organic waste utilization for biorefineries. *Renew. Sustain. Energy Rev.* **2015**, *49*, 335–349. [CrossRef]
18. Rivero, C.P.; Hu, Y.; Kwan, T.H.; Webb, C.; Theodoropoulos, C.; Daoud, W.; Lin, C.S.K. 1-Bioplastics from solid waste. In *Current Developments in Biotechnology and Bioengineering, Solid Waste Management*, 1st ed.; Wong, J.W.C., Tyagi, R.D., Pandey, A., Eds.; Elsevier: Amsterdam, The Netherlands, 2017; pp. 1–26, ISBN 9780444636652.
19. Dietrich, K.; Dumont, M.-J.; Del Rio, L.F.; Orsat, V. Producing PHAs in the bioeconomy—Towards a sustainable bioplastics. *Sustain. Prod. Consum.* **2017**, *9*, 58–70. [CrossRef]

20. Franzoso, F.; Vaca-Garcia, C.; Rouilly, A.; Evon, P.; Montoneri, E.; Persico, P.; Mendichi, R.; Nisticò, R.; Francavilla, M. Extruded versus solvent cast blends of poly(vinyl alcohol-co-ethylene) and biopolymers isolated from municipal biowaste. *J. Appl. Polym. Sci.* **2016**, *133*, 43009–43025. [CrossRef]

21. Nisticò, R.; Evon, P.; Labonne, L.; Vaca-Medina, G.; Montoneri, E.; Francavilla, M.; Vaca-Garcia, C.; Magnacca, G.; Franzoso, F.; Negre, M. Extruded poly(ethylene-co-vinyl alcohol) composite films containing biopolymers isolated from municipal biowaste. *ChemistrySelect* **2016**, *1*, 2354–2365. [CrossRef]

22. Xu, S.; Liu, C.; Wiezorek, J. 20 renewable biowastes derived carbon materials as green counter electrodes for dye-sensitized solar cells. *Mater. Chem. Phys.* **2018**, *204*, 294–304. [CrossRef]

23. Narzani, R.; Bordoloi, N.; Sarma, B.; Gogoi, L.; Gogoi, N.; Borkotoki, B.; Kataki, R. Fabrication of biochars obtained from valorization of biowaste and evaluation of its physicochemical properties. *Bioresour. Technol.* **2017**, *242*, 324–328. [CrossRef] [PubMed]

24. Qambrani, N.A.; Rahman, M.M.; Won, S.; Shim, S.; Ra, C. Biochar properties and eco-friendly applications for climate change mitigation, waste management, and wastewater treatment: A review. *Renew. Sustain. Energy Rev.* **2017**, *79*, 255–273. [CrossRef]

25. Magnacca, G.; Guerretta, F.; Vizintin, A.; Benzi, P.; Valsania, M.C.; Nisticò, R. Preparation, characterization and environmental/electrochemical energy storage testing of low-cost biochar from natural chitin obtained via pyrolysis at mild conditions. *Appl. Surf. Sci.* **2018**, *427*, 883–893. [CrossRef]

26. Chen, P.; Xie, Q.; Addy, M.; Zhou, W.; Liu, Y.; Wang, Y.; Cheng, Y.; Li, K.; Ruan, R. Utilization of municipal solid and liquid wastes for bioenergy and bioproducts production. *Bioresour. Technol.* **2016**, *215*, 163–172. [CrossRef] [PubMed]

27. Vakalis, S.; Sotiropoulos, A.; Moustakes, K.; Malamis, D.; Vekkos, K.; Baratieri, M. Thermochemical valorization and characterization of household biowaste. *J. Environ. Manag.* **2017**, *203*, 648–654. [CrossRef] [PubMed]

28. Beauchet, R.; Monteul-Rivera, F.; Lavoie, J.M. Conversion of lignin to aromatic-based chemicals (L-chems) and biofuels (L-fuels). *Bioresour. Technol.* **2012**, *121*, 328–334. [CrossRef] [PubMed]

29. Ardolino, F.; Parrillo, F.; Arena, U. Biowaste-to-biomethane or biowaste-to-energy? An LCA study on anaerobic digestion of organic waste. *J. Clean. Prod.* **2018**, *174*, 462–476. [CrossRef]

30. Zhao, X.; Wei, L.; Cheng, S.; Julson, J. Review of heterogeneous catalysts for catalytically upgrading vegetable oils into hydrocarbon biofuels. *Catalysts* **2017**, *7*, 83. [CrossRef]

31. Montoneri, E.; Mainero, D.; Boffa, V.; Perrone, D.G.; Montoneri, C. Biochemenergy: A project to turn an urban wastes treatment plant into biorefinery for the production of energy, chemicals and consumer's products with friendly environmental impact. *Int. J. Glob. Environ. Issues* **2011**, *11*, 170–196. [CrossRef]

32. Montoneri, E.; Bianco Prevot, A.; Avetta, P.; Arques, A.; Carlos, L.; Magnacca, G.; Laurenti, E.; Tabasso, S. Food wastes conversion to products for use in chemical and environmental technology, material science and agriculture. In *The Economic Utilisation of Food Co-Products*; Kazmi, A., Shuttleworth, P., Eds.; Royal Society of Chemistry Publishing: Cambridge, UK, 2013; pp. 64–109, ISBN 978-1-84973-615-2.

33. Montoneri, E.; Boffa, V.; Savarino, P.; Perrone, D.; Ghezzo, M.; Montoneri, C.; Mendichi, R. Acid soluble bio-organic substances isolated from urban bio-waste. Chemical composition and properties of products. *Waste Manag.* **2011**, *31*, 10–17. [CrossRef] [PubMed]

34. Nisticò, R.; Cesano, F.; Franzoso, F.; Magnacca, G.; Scarano, D.; Funes, I.G.; Carlos, L.; Parolo, M.E. From biowaste to magnet-responsive materials for water remediation from polycyclic aromatic hydrocarbons. *Chemosphere* **2018**, *202*, 686–693. [CrossRef] [PubMed]

35. Nisticò, R.; Barrasso, M.; Carrillo Le Roux, G.A.; Seckler, M.M.; Sousa, W.; Malandrino, M.; Magnacca, G. Biopolymers from composted biowaste as stabilizers for the synthesis of spherical and homogeneously sized silver nanoparticles for textile applications on natural fibers. *ChemPhysChem* **2015**, *16*, 3902–3909. [CrossRef] [PubMed]

36. Vargas, A.K.N.; Bianco Prevot, A.; Montoneri, E.; Le Roux, G.C.; Savarino, P.; Cavalli, R.; Guardani, R.; Tabasso, S. Use of biowaste-derived biosurfactants in production of emulsions for industrial use. *Ind. Eng. Chem. Res.* **2014**, *53*, 8621–8629. [CrossRef]

37. Montoneri, E.; Boffa, V.; Savarino, P.; Tambone, F.; Adani, F.; Micheletti, L.; Gianotti, C.; Chiono, R. Use of biosurfactants from urban wastes compost in textile dyeing and soil remediation. *Waste Manag.* **2009**, *29*, 383–389. [CrossRef] [PubMed]

38. Savarino, P.; Montoneri, E.; Bottigliengo, S.; Boffa, V.; Guizzetti, T.; Perrone, D.G.; Mendichi, R. Biosurfactants from urban wastes as auxiliaries for textile dyeing. *Ind. Eng. Chem. Res.* **2009**, *48*, 3738–3748. [CrossRef]

39. Bianco Prevot, A.; Baino, F.; Fabbri, D.; Franzoso, F.; Magnacca, G.; Nisticò, R.; Arques, A. Urban biowaste-derived sensitizing materials for caffeine photodegradation. *Environ. Sci. Pollut. Res.* **2017**, *24*, 12599–12607. [CrossRef] [PubMed]

40. Avetta, P.; Bella, F.; Bianco Prevot, A.; Laurenti, E.; Montoneri, E.; Arques, A.; Carlos, L. Waste cleaning waste: Photodegradation of monochlorophenols in the presence of waste derived organic catalysts. *ACS Sustain. Chem. Eng.* **2013**, *1*, 1545–1550. [CrossRef]

41. Richardson, S.D.; Ternes, T.A. Water analysis: Emerging contaminants and current issues. *Anal. Chem.* **2014**, *86*, 2813–2848. [CrossRef] [PubMed]

42. Franzoso, F.; Nisticò, R.; Cesano, F.; Corazzari, I.; Turci, F.; Scarano, D.; Bianco Prevot, A.; Magnacca, G.; Carlos, L.; Martire, D.O. Biowaste-derived substances as a tool for obtaining magnet-sensitive materials for environmental applications in wastewater treatments. *Chem. Eng. J.* **2017**, *310*, 307–316. [CrossRef]

43. Klamerth, N.; Malato, S.; Maldonado, M.I.; Aguera, A.; Fernández-Alba, A.R. Application of photo-Fenton as a tertiary treatment of emerging contaminants in municipal wastewater. *Environ. Sci. Technol.* **2010**, *44*, 1792–1798. [CrossRef] [PubMed]

44. Zapata, A.; Oller, I.; Rizzo, L.; Hilgert, S.; Maldonado, M.I.; Sánches-Pérez, J.A.; Malato, S. Evaluation of operating parameters involved in solar photo-Fenton treatment of wastewater: Interdependence of initial pollutant concentration, temperature and iron concentration. *Appl. Catal. B* **2010**, *97*, 292–298. [CrossRef]

45. Klamerth, N.; Rizzo, L.; Malato, S.; Maldonado, M.I.; Aguera, A.; Fernández-Alba, A.R. Degradation of fifteen emerging contaminants at $\mu g L^{-1}$ initial concentrations by mild solar photo-Fenton in MWTP effluents. *Water Res.* **2010**, *44*, 545–554. [CrossRef] [PubMed]

46. Demarchis, L.; Minella, M.; Nisticò, R.; Maurino, V.; Minero, C.; Vione, D. Photo-Fenton reaction in the presence of morphologically controlled hematite as iron source. *J. Photochem. Photobiol. A* **2015**, *307–308*, 99–107. [CrossRef]

47. Bauer, R.; Fallmann, H. The photo-Fenton oxidation—A cheap and efficient wastewater treatment method. *Res. Chem. Intermed.* **1997**, *23*, 341–354. [CrossRef]

48. Lacombe, S.; Pigot, T. Materials for selective photo-oxygenation vs. photocatalysis: Preparation, properties and applications in environmental and health fields. *Catal. Sci. Technol.* **2016**, *6*, 1571–1592. [CrossRef]

49. Bethi, B.; Sonawane, S.H.; Bhanvase, B.A.; Gumfekar, S.P. Nanomaterials-based advanced oxidation processes for wastewater treatment: A review. *Chem. Eng. Process.* **2016**, *109*, 178–189. [CrossRef]

50. Vaughan, P.P.; Blough, N.V. Photochemical formation of hydroxyl radical by constituents of natural waters. *Environ. Sci. Technol.* **1998**, *32*, 2947–2953. [CrossRef]

51. Canonica, S. Oxidation of aquatic organic contaminants induced by excited triplet states. *CHIMIA Int. J. Chem.* **2007**, *61*, 641–644. [CrossRef]

52. Moonshine, M.; Rudich, Y.; Katsman, S.; Graber, E.R. Atmospheric HULIS enhance pollutant degradation by promoting the dark Fenton reaction. *Geophys. Res. Lett.* **2008**, *25*, L20807. [CrossRef]

53. Sodano, M.; Lerda, C.; Nisticò, R.; Martin, M.; Magnacca, G.; Celi, L.; Said-Pullicino, D. Dissolved organic carbon retention by coprecipitation during the oxidation of ferrous iron. *Geoderma* **2017**, *307*, 19–29. [CrossRef]

54. Weishaar, J.L.; Aiken, G.R.; Bergamaschi, B.A.; Fram, M.S.; Fujii, R.; Mopper, K. Evaluation of specific ultraviolet absorbance as an indicator of the chemical composition and reactivity of dissolved organic carbon. *Environ. Sci. Technol.* **2003**, *37*, 4702–4708. [CrossRef] [PubMed]

55. Wu, M.; Song, M.; Liu, M.; Jiang, C.; Li, Z. Fungicidal activities of soil humic/fulvic acids as related to their chemical structures in greenhouse vegetable fields with cultivation chronosequence. *Sci. Rep.* **2016**, *6*, 32858. [CrossRef] [PubMed]

56. Celi, L.; Schnitzer, M.; Negre, M. Analysis of the carboxyl groups in soil humic acids by a wet chemical method, Fourier-transform infrared spectrophotometry, and solution-state carbon-13 nuclear magnetic resonance. A comparative study. *Soil Sci.* **1997**, *162*, 189–197. [CrossRef]

57. Montoneri, E.; Boffa, V.; Savarino, P.; Perrone, D.G.; Musso, G.; Mendichi, R.; Chierotti, M.R.; Gobetto, R. Biosurfactants from urban green waste. *ChemSusChem* **2009**, *2*, 239–247. [CrossRef] [PubMed]

58. Ranatunga, T.D.; He, Z.; Bhat, K.N.; Zhong, J. Solid-state ^{13}C nuclear magnetic resonance spectroscopic characterization of soil organic matter fractions in a forest ecosystem subjected to prescribed burning and thinning. *Pedosphere* **2017**, *27*, 901–911. [CrossRef]

59. Albrecht, R.; Ziarelli, F.; Alarcon-Gutierrez, E.; Le Petit, J.; Terrom, G.; Perissol, C. ^{13}C solid-state NMR assessment of decomposition pattern during co-composting of sewage sludge and green wastes. *Eur. J. Soil Sci.* **2008**, *59*, 445–452. [CrossRef]

60. Bonifacio, E.; Petrillo, M.; Petrella, F.; Tambone, F.; Celi, L. Alien red oak affects soil organic matter cycling and nutrient availability in low-fertility well-developed soils. *Plant Soil* **2015**, *395*, 215–229. [CrossRef]

61. Montoneri, E.; Tomasso, L.; Colajanni, N.; Zelano, I.; Alberi, F.; Cossa, G.; Barberis, R. Urban wastes to remediate industrial sites: A case of polycyclic aromatic hydrocarbons contamination and a new process. *Int. J. Environ. Sci. Technol.* **2014**, *11*, 251–262. [CrossRef]

62. Carlos, L.; Pedersen, B.W.; Ogilby, P.R.; Martire, D.O. The role of humic acid aggregation on the kinetics of photosensitized singlet oxygen production and decay. *Photochem. Photobiol. Sci.* **2011**, *10*, 1080–1086. [CrossRef] [PubMed]

63. Gomis, J.; Bianco Prevot, A.; Montoneri, E.; Gonzalez, M.C.; Amat, A.M.; Martire, D.O.; Arques, A.; Carlos, L. Waste sourced bio-based substances for solar-driven wastewater remediation: Photodegradation of emerging pollutants. *Chem. Eng. J.* **2014**, *235*, 236–243. [CrossRef]

64. Bianco Prevot, A.; Avetta, P.; Fabbri, D.; Laurenti, E.; Marchis, T.; Perrone, D.G.; Montoneri, E.; Boffa, V. Waste derived bio-organic substances for light induced generation of reactive oxygenated species. *ChemSusChem* **2011**, *4*, 85–90. [CrossRef] [PubMed]

65. Voelker, B.M.; Sulzberger, B. Effects of fulvic acid on Fe(II) oxidation by hydrogen peroxide. *Environ. Sci. Technol.* **1996**, *30*, 1106–1114. [CrossRef]

66. Huang, W.; Brigante, M.; Wu, F.; Hanna, K.; Mailhot, G. Development of a new homogenous photo-Fenton process using Fe(III)–EDDS complexes. *J. Photochem. Photobiol. A* **2012**, *239*, 17–23. [CrossRef]

67. Florawiva Compost di Qualità. Available online: http://ambiente.aceapinerolese.it/florawiva-compost/ (accessed on 6 May 2017).

68. Swift, R.S. Organic matter characterization, Chapter 35. In *Book: Methods of Soil Analysis Part 3—Chemical Methods, SSSA Book Series 5.3, 1996*; Spark, D.L., Page, A.L., Helmke, P.A., Loeppert, R.H., Soltanpour, P.N., Tabatabai, M.A., Johnston, C.T., Summer, M.E., Eds.; Soil Science Society of America: Madison, WI, USA, 1996; pp. 1018–1020.